Naval Surface Warfare Center
Carderock Division
West Bethesda, MD 20817-5700

NSWCCD-50-TR–2007/064 September 2007

Hydromechanics Department Report

Thrust Breakdown Characteristics of Conventional Propellers

by

Scott D. Black

NSWCCD-50-TR–2007/064 Thrust Breakdown Characteristics of Conventional Propellers

REPORT DOCUMENTATION PAGE

Form Approved
OMB No. 0704-0188

1. AGENCY USE ONLY (*Leave Blank*)	2. REPORT DATE	3. REPORT TYPE AND DATES COVERED
	September 2007	Final, September 2007

4. TITLE AND SUBTITLE
Thrust Breakdown Characteristics of Conventional Propellers

5. FUNDING NUMBERS
07-1-2125-146

6. AUTHOR(S)
Scott D. Black

7. PERFORMING ORGANIZATION NAME(S) AND ADDRESS(ES)
Propulsion and Fluid Systems Division, Code 5400
NSWC, Carderock Division
9500 MacArthur Blvd.
West Bethesda, MD 20817-5700

8. PERFORMING ORGANIZATION REPORT NUMBER
NSWCCD-50-TR-2007/064

9. SPONSORING / MONITORING AGENCY NAME(S) AND ADDRESS(ES)
Commander, PMS 385
Naval Sea Systems Command
1333 Isaac Hull Ave, SE
Washington Navy Yard, DC 20375-2501

10. SPONSORING / MONITORING AGENCY REPORT NUMBER

11. SUPPLEMENTARY NOTES

12.a DISTRIBUTION / AVAILIBILITY STATEMENT
Approved for Public Release; distribution is unlimited

12.b DISTRIBUTION CODE

13. ABSTRACT (*Maximum 200 words*)

Historically, the Burrill diagram has been used early in the propeller design process to estimate the inception of thrust loss due to cavitation. That data was based on a systematic series of propeller tested in a uniform inflow. This report develops an alternative set of curves based on five modern propeller designs to estimate thrust breakdown for both uniform inflow and for a range of non-uniformities.

16. SUBJECT TERMS	15. NUMBER OF PAGES
PROPELLERS	52
	16. PRICE CODE

17. SECURITY CLASSIFICATION OF REPORT	18. SECURITY CLASSIFICATION OF THIS PAGE	19. SECURITY CLASSIFICATION OF ABSTRACT	20. LIMITATION OF ABSTRACT
UNCLASSIFIED	UNCLASSIFIED	UNCLASSIFIED	SAME AS REPORT

(THIS PAGE INTENTIONALLY LEFT BLANK)

CONTENTS

LIST OF TABLES

LIST OF FIGURES

Page

NOMENCLATURE

A_P	Projected blade area
C	Chord length
D	Diameter
EAR	Expanded area ratio
g	Gravitational constant
h	Depth of submergence at shaft centerline
IA	Incidence angle (degrees)
J_A	Propeller advance coefficient, $\frac{V_S(1-w_T)}{nD}$
J_S	Ship advance coefficient, V_S/nD
K_T	Thrust coefficient, $\frac{T}{\rho n^2 D^4}$
n	Revolutions per second
N	Revolutions per minute
P	Pitch
PAR	Projected area ratio
p_0	Atmospheric pressure
p_v	Vapor pressure
q_T	Dynamic pressure, $q_T = \frac{1}{2}\rho\left(V_A^2 + (0.7\pi nD)^2\right)$
r	Propeller radius at a section
R	Overall propeller radius
t	Thrust deduction
T	Thrust
V_A	Axial velocity in propeller plane, $V_A = V_S(1-w_T)$
V_{rel}	Relative velocity
V_S	Ship speed
w_T	Taylor wake fraction
x	Rake
Z	Number of blades
θ	Skew
ρ	Mass density

σ	Cavitation number based on ship speed, $\frac{p_0 - p_v + \rho g h}{\frac{1}{2}\rho V_s^2}$
σ_n	Cavitation number based on rpm, $\frac{p_0 - p_v + \rho g h}{\frac{1}{2}\rho (nD)^2}$
$\sigma_{0.7R}$	Burrill cavitation number, $\frac{p_0 - p_v + \rho g h}{\frac{1}{2}\rho \left(V_A^2 + (0.7\pi nD)^2\right)}$
τ_c	Burrill thrust loading coefficient, $\frac{Thrust}{\frac{1}{2}\rho A_P \left(V_A^2 + (0.7\pi nD)^2\right)}$

ABBREVIATIONS

CAV	Cavitating (subscript)
CRP	Controllable-Reversible Pitch
EAR	Expanded Area Ratio
EHP	Effective Horsepower
FPP	Fixed-Pitch Propeller
kt.	knot, 1.6878 ft/sec (0.5144 m/s)
NSWCCD	Naval Surface Warfare Center, Carderock Division
PAR	Projected Area Ratio
RPM	Revolutions per minute
WET	Non-cavitating (subscript)

ABSTRACT

Historically, the Burrill diagram has been used early in the propeller design process to estimate the inception of thrust loss due to cavitation. This report develops an alternative set of curves based on five modern propeller designs to estimate thrust breakdown for both uniform inflow and for a range of non-uniformities. A recommended blade area ratio relation is developed for uniform flow designs. This relation falls very close to the Burrill 15% back cavitation contour. A relationship to adjust that curve to account for non-uniform inflows is also derived.

ADMINISTRATIVE INFORMATION

The hydrodynamic analysis reported herein was performed by the Naval Surface Warfare Center, Carderock Division (NSWCCD), Hydrodynamics Department, Propulsor and Fluid System Division, Code 5400. The work was sponsored by Naval Sea Systems Command, PMS 385, under work unit 07-1-2125-146 between January and August of 2007.

INTRODUCTION

Thrust breakdown is defined by the International Towing Tank Conference [1] as:

The phenomenon of loss of thrust due to excessive cavitation on a sub-cavitating type propeller. The torque absorbed by the propeller is affected similarly and is called torque breakdown. Both the thrust and torque coefficients may increase slightly above non-cavitating values near the initial inception of cavitation. In general, the changes in thrust and torque are such that propeller efficiency is reduced.

Propellers can experience thrust loss due to cavitation when they are operating at high speeds, low pressures or wide angle of attack variations. Thrust breakdown is often defined as a 1% loss of thrust relative to the non-cavitating thrust. Increased RPM is needed to achieve the required thrust to recover from thrust breakdown.

Typically, some percentage of the blade area can be covered with cavitation without measurable thrust loss. The Burrill chart, shown in Figure 1, has been used as a guide for how much blade area is required to avoid thrust loss at a full power condition [2]. Typically, if the full power operating point falls on or below the 10% back cavitation curve, no measurable thrust

breakdown is observed. This curve is similar to Burrill's 1943 curve for warships with special sections [3].

Cavitation is detrimental because it can lead to thrust breakdown, vibration, noise, erosion and blade damage. Propellers operating with enough cavitation to cause thrust breakdown can experience structural damage in the form of erosion or bent trailing edges. Bent trailing edges are generally attributed to propeller blade sheet cavitation that extends beyond the trailing edge of the blade. These sheets violently collapse as the blade moves out of the wake deficit produced by the hull.

This report describes a study done to develop a new criterion to estimate the onset of thrust breakdown. It investigates the performance of five modern propeller designs to develop a method to estimate the inception of thrust breakdown. This study was done for propellers operating in both uniform and non-uniform inflow.

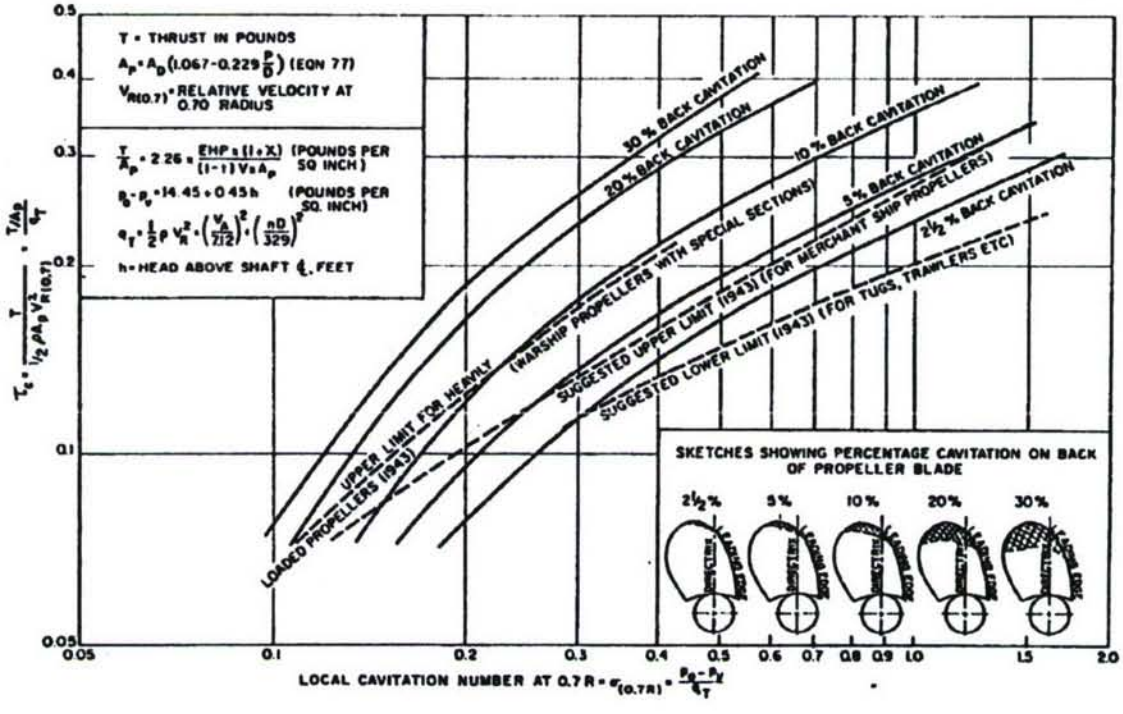

Figure 1. Burrill diagram.

BACKGROUND

Parsons and Cook [4] and Barnaby [5] performed cavitation tests on both models and full scale ships. They concluded that extreme back or face cavitation causing thrust breakdown could be avoided by increasing the blade surface area. Criteria were subsequently developed that relate the "Mean Thrust" to the required "Blade Surface Area" in the form of a limiting thrust loading coefficient. In 1943, Burrill developed a criteria based on thrust loading and cavitation number

that had reasonable agreement with his experimental data [3]. In 1963, Burrill updated his criteria with curves of percentage back cavitation contours [2]. Most propellers are designed to operate below the 10% back cavitation line on the 1963 Burrill chart. Some additional thrust breakdown curves were developed by Gawn and Burrill [6] and SSPA [7] and are shown in Figure 2. The Gawn and Burrill curve corresponded to Burrill's heavily loaded propeller curve from 1943.

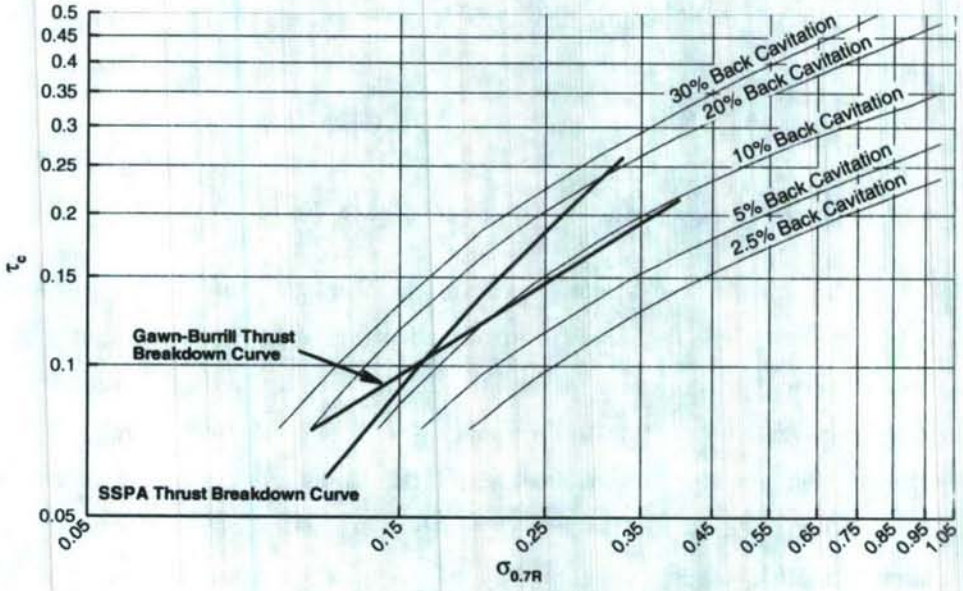

Figure 2. Gawn-Burrill and SSPA thrust breakdown criteria.

The percent back cavitation curves on the Burrill chart are based on a systematic series of propellers tested in uniform flow for a range of cavitation numbers. Therefore, the effects of non-uniformities in the inflow are not present in the Burrill back cavitation curves. The 1943 Burrill curves along with the Gawn-Burrill and SSPA curves are based on model and full scale propellers operating on real ship arrangements.

OBJECTIVE

Recent designs for both naval and commercial applications have moved away from standard airfoil blade sections to "advanced blade sections" that are custom designed to delay the onset of blade surface cavitation and thrust breakdown [8]. Advanced blade sections have chord-wise load and thickness distributions that increase the blade surface cavitation inception speed.

Propellers designed to operate in a uniform inflow can have different blade sections than those designed to operate in a non-uniform inflow. The thickness of the propeller blade is primarily driven by structural strength, cavitation inception, and for special cases, acoustic

requirements. As discussed by Brockett [9], thin blade sections can operate at very low cavitation numbers without cavitation inception if they experience little angle of attack variation. Thicker sections can generally sustain larger angle of attack variations without cavitation inception, but have earlier back bubble cavitation inception at higher speeds.

Recent designs have been able to exceed the thrust breakdown lines on the Burrill diagram. The success of these designs indicates that the thrust breakdown criterion needs to be re-evaluated. Modern blade section design, manufacturing and design tools allow current designs to perform better than the propellers used to develop the existing criteria.

APPROACH

THRUST BREAKDOWN ANALYSIS TOOLS

A number of tools have been developed that can compute the thrust loss due to cavitation on a propeller. These tools can be broadly classified as potential flow codes, such as lifting-surface or panel methods, and viscous flow codes like Reynolds-Averaged Navier-Stokes (RANS) solvers. One lifting-surface analysis tool for predicting cavitation is the MPUF-3a software being developed by Kinnas et al. [10]. Kinnas is also leading a team that is developing a panel method solver called PROPCAV [11,12]. Another unsteady panel method analysis tool, called PROCAL, is being developed by the Cooperative Research: Ships (CRS) consortium [13]. Several RANS flow codes have the capability to simulate cavitating flows on propellers. One of these RANS flow codes is derived from the UNCLE software developed at the Mississippi State University, which has been extended to predict two-phase flows at the Applied Research Laboratory at Pennsylvania State University (ARL/PSU) [14]. The commercial RANS software FLUENT, has also been used to compute cavitating propeller performance [15, 16].

Viscous flow codes have the potential to achieve more accurate cavitating propeller analysis than potential flow solvers. However, at this time they are too slow to do unsteady cavitating propeller analysis for a wide range of advance coefficients, cavitation numbers and inflow conditions. Also, the amount of thrust loss due to cavitation versus experiments was not consistently predicted for the sample cases in the published papers. The PROCAL software is still under development, so it was not considered as a tool for this project. Validation exercises performed by the software developers of MPUF-3a and PROPCAV, have shown that PROPCAV provides better correlation to experimental data than MPUF-3a [11]. Therefore, the PROPCAV software was used for this project.

SAMPLE PROPELLERS

Five propellers were used in this study to develop a new thrust breakdown criterion. All five designs have non-standard blade sections. These Eppler-Shen blade sections were custom designed to delay blade surface cavitation [8, 17, 18]. All of the propellers were designed to operate on ships that have an inclined, exposed shaft-line supported by struts. Two of the propellers are controllable pitch designs while the other three are fixed pitch. The propeller geometries are provided in Appendix A.

The use of five real propeller designs in this study has both strengths and weaknesses. Because the designs are for real naval propellers, they are geometries developed from realistic requirements on cavitation inception, efficiency, unsteady forces, mechanical and structural characteristics. Because these propellers were designed for specific non-uniform inflows, their performance in different inflows may not be representative of their performance in their design inflows.

The propellers were tested in either the NSWCCD 36" variable pressure water tunnel or the NSWCCD Large Cavitation Channel. The full power condition for each of the propellers is shown in the Burrill chart in Figure 3. The thrust breakdown experiments in the water tunnel were performed at a shaft angle representative of the flow inclination of the propeller on the full scale installation.

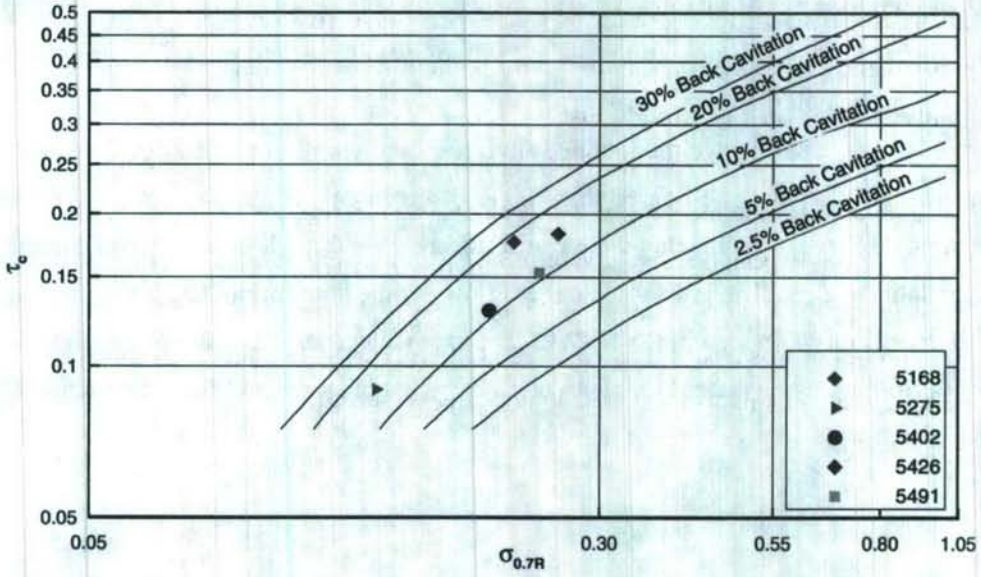

Figure 3. Full power operating points of sample propellers on the Burrill chart.

OPEN WATER VALIDATION

PROPCAV was used to predict the open water characteristics of the propellers for a range of advance coefficients. The PROPCAV predictions are compared to the open water tests

and the results are provided in Appendix B. Table 1 shows the errors from PROPCAV at the full power advance coefficient. Calculations were performed with fifty panels chord-wise and thirty panels span-wise, which is the resolution used for the subsequent thrust breakdown calculations. In general, the software significantly under-predicts the open water thrust and torque.

Table 1. Open water performance at full power advance coefficient from PROPCAV.

Propeller	Full Power J_A	K_T error	K_Q error
5168	1.20	-4.4%	-0.7%
5275	1.23	-0.5%	+2.4%
5402	0.86	-7.4%	-6.5%
5426	0.78	-5.8%	-5.9%
5491	1.04	-8.5%	-8.5%

THRUST BREAKDOWN VALIDATION

The PROPCAV software was exercised to see how well it could predict the experimental thrust breakdown performance for the five propeller geometries. The calculations were performed using a thrust identity condition similar to what was used in the experiments. The advance coefficient was adjusted so that the calculated non-cavitating thrust matched the experimental non-cavitating thrust. The cavitating analysis determined the amount of thrust loss relative to the non-cavitating thrust.

A wake survey for the inclined shaft test configuration in the NSWCCD 36" water tunnel was available for the nine-degree shaft angle arrangement. A sample test setup is shown in Figure 4. For experiments that were run at different shaft angles, the harmonic content of the wake data were modified to simulate the inflow for the appropriate test inclination angles. The 5491 propeller was tested in the NSWCCD Large Cavitation Channel. A nominal wake survey was performed using Laser Doppler Velocimetry, which was used for the validation of the 5491 propeller.

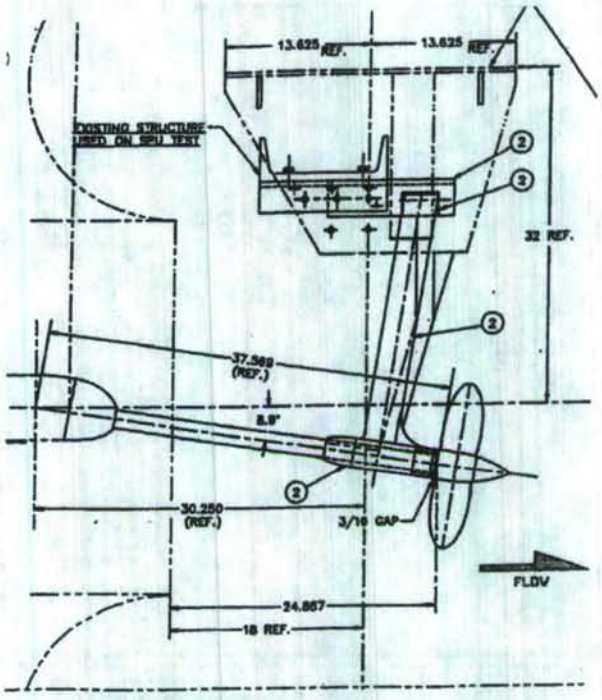

Figure 4. NSWCCD water tunnel inclined shaft test arrangement.

REDUCED HARMONIC MODELING

Early in the ship design process, the detailed inflow characteristics of the propeller are not known. However, quantities like the hydrodynamic shaft angle and boundary layer ingestion can be used to estimate a preliminary inflow that contains the dominant harmonics. An investigation was performed to determine how many harmonics of inflow are necessary to adequately predict the thrust breakdown performance of a propeller.

For the 5491 propeller, inflows with sixteen-, four- and two-harmonics were used for the cavitation analysis. As shown in Figure 5, the 5491 results were nearly identical in all cases. For the 5275 propeller, inflows with sixteen- and two-harmonics were used. The 5275 results fell within 0.5% of each other for thrust loss at the full power condition.

These results show that while inflows with higher harmonic may be needed to define cavitation inception, the use of fewer harmonics provides satisfactory thrust loss predictions. Therefore, the dependence of thrust breakdown on inflow angle is relevant even for inflows that have significantly higher harmonic contents.

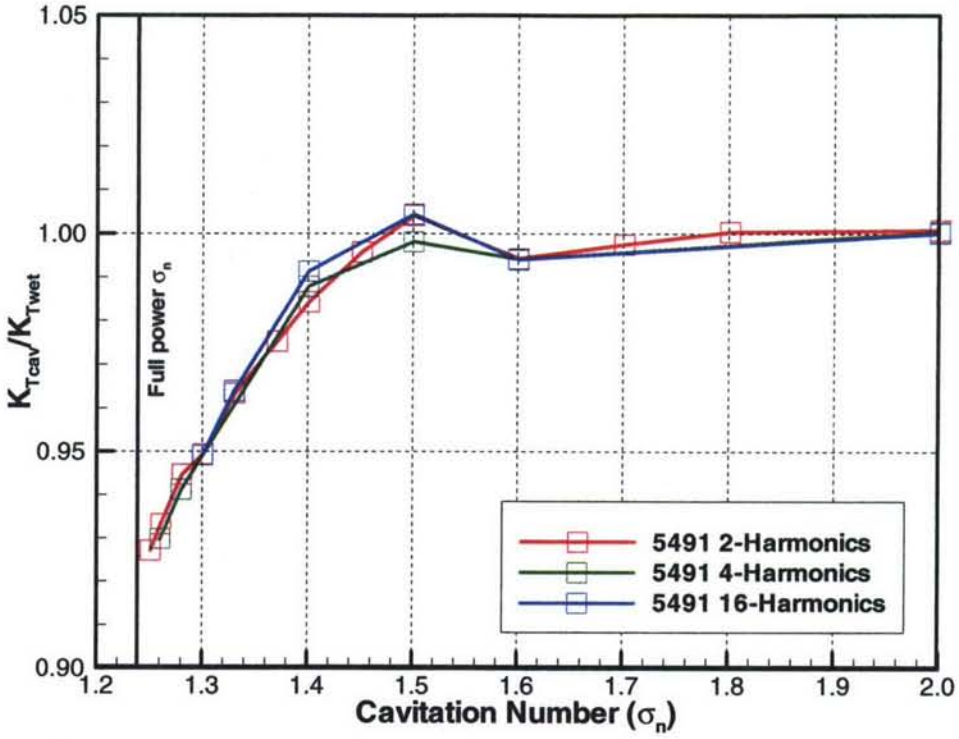

Figure 5. Sensitivity of thrust reduction to harmonic content in wake (Prop 5491).

Propeller 5168

During water tunnel experiments, the 5168 propeller was tested in an inclined shaft configuration with an 8.9 degree shaft angle. At a cavitation number (σ_n) of 1.632 and thrust coefficient (K_T) of 0.289, a thrust loss of 4.5% was measured. Calculations predicted a 4.1% thrust loss at full power. The calculations were done using an inflow measured for a nine-degree shaft inclination.

Propeller 5275

During water tunnel experiments, the 5275 propeller was tested in an inclined shaft configuration with a 6.1 degree shaft angle. This propeller was tested at three different reference pressures for a range of speeds. PROPCAV did not converge at the lowest cavitation number (highest speed) for the two lowest pressures. A comparison of the thrust loss at the highest and lowest pressures is shown in Figure 6. At a tunnel pressure of 17.0 psi, the code does a good job predicting the experimental results. At the lower pressure conditions, the code under-predicts the thrust loss. These calculations were performed using a two-harmonic wake. The calculations that were done with sixteen harmonics at the 17.0 psi condition were within 0.5 percent of the 2-harmonic results.

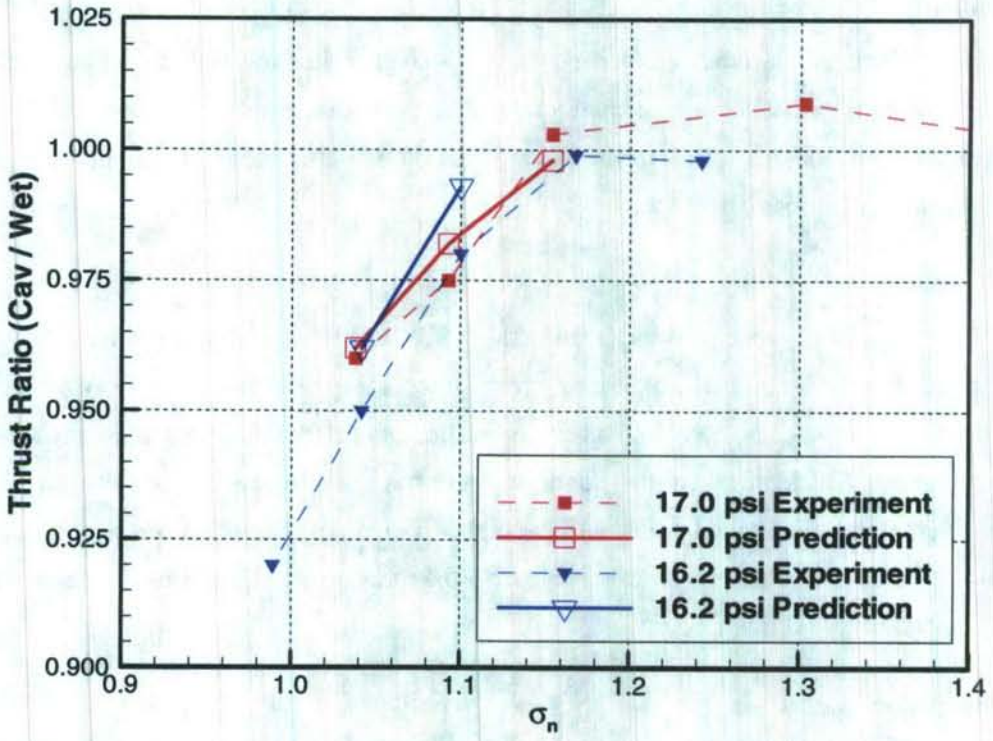

Figure 6. Comparison of experimental and predicted thrust loss for propeller 5275.

Propeller 5402

During water tunnel experiments, the 5402 propeller was tested in an inclined shaft configuration with a 9.1 degree shaft angle. At a cavitation number of 0.917 and thrust coefficient of 0.182, no thrust loss was measured in the water tunnel. Using a two-harmonic inflow, the computed thrust loss was 14%. The predicted cavitation pattern, shown in Figure 7, shows much more cavitation is predicted than was observed during the experiment.

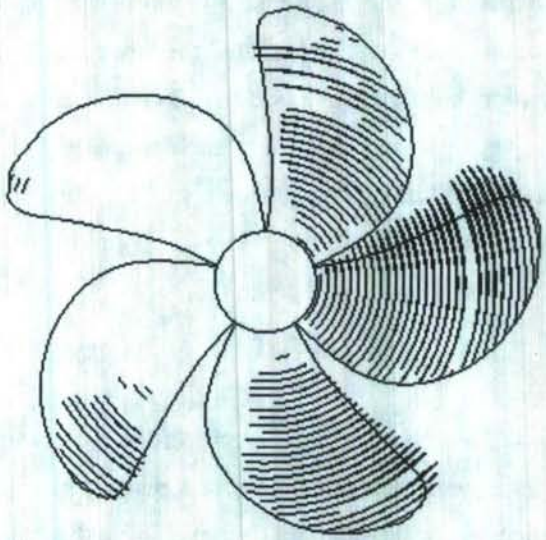

Figure 7. Predicted cavitation pattern on Propeller 5402 at full power.

Propeller 5426

During water tunnel experiments, the 5426 propeller was tested in an inclined shaft configuration with a 9.2 degree shaft angle. At a cavitation number of 1.069 and thrust coefficient of 0.230, a 1.75% thrust loss was measured. Using a two-harmonic inflow, the computed thrust loss was 9.3%.

Propeller 5491

The 5491 propeller was tested in the NSWCCD large cavitation channel behind a fully appended hull. A nominal wake survey for that test setup was used for the cavitation analysis. At a cavitation number of 1.239 and advance coefficient of 0.228, no thrust loss was measured in the experiment. Calculations for this condition were run using inflows having sixteen-, four- and two-harmonics. The calculations with the higher harmonics did not converge at the cavitation number used in the test. As shown in Figure 5 the thrust loss extrapolates to between eight and nine percent for all three inflows.

Validation Conclusions

The PROPCAV software was found to be significantly conservative for almost all cases. The code predicted more thrust loss than was actually measured during experiments. The only exception was the 5275 propeller, where the software predicted about 1% less thrust loss than was measured for the low pressure condition.

THRUST BREAKDOWN SENSITIVITY

Thrust breakdown calculations were performed using fifty panels in the chord-wise direction and thirty panels in the span-wise direction. The hub was paneled as a cylindrical shaft. The unsteady propeller forces were computed for three revolutions in the non-cavitating condition and six revolutions for the cavitating condition. The propeller time step was set at nine degrees, creating forty time steps per revolution. For each propeller, calculations were typically run for ten cavitation numbers and ten advance coefficients to develop maps showing where the propeller experienced thrust loss due to cavitation. The full contour maps produced by the uniform and non-uniform inflows are shown in Appendix C.

DESIGN FLOW

Calculations for the five sample propellers were performed for a range of cavitation numbers and advance coefficients using each propeller's circumferential mean design inflow. Since these propellers are wake-adapted designs, doing the calculations using a uniform inflow

would not result in representative performance. Calculations were done for a range of advance coefficients starting at approximately sixty percent of the design value and extending to ten percent above the design value. Performing calculations with an advance coefficient greater than ten percent above the design value resulted in pressure side cavitation, which was not the form of thrust breakdown being studied in this program. Calculations were performed at decreasing cavitation numbers until the software failed to converge, which typically occurred when more than five to ten percent thrust loss was predicted.

To achieve good cavitation characteristics in non-uniform flow, the blade sections of these propellers have chord-wise loading and thickness distributions designed to avoid cavitation over a range of angles of attack. Because these designs were developed to operate in non-uniform inflows, their thrust breakdown performance is worse than what could be achieved by a propeller designed to operate in a uniform inflow.

The results of the calculations were compiled and converted into thrust (τ_c) and cavitation number (σ_n) coefficients. Contours are located where each of the propellers began to experience more than a two-percent thrust loss. The two-percent criteria was used because, when running PROPCAV, unless a high number of iterations were used, the non-cavitating and cavitating unsteady forces, could be off by up to one-percent. By using a two-percent criterion, the code convergence uncertainty was suppressed.

Figure 8 shows the zero-degree inclination data with the two-percent thrust breakdown curves. The horizontal lines show the full power operating thrust coefficient values the particular designs were developed for. The symbols show where each propeller has a two-percent thrust breakdown at it's corresponding full power thrust coefficient. For each propeller, the off-design performance tails off to the upper right. This shows how far off-design the propeller can operate before suffering thrust breakdown. The symbols reflect the actual performance of the designs in an on-design condition. The on-design condition is used to develop the new thrust breakdown criteria.

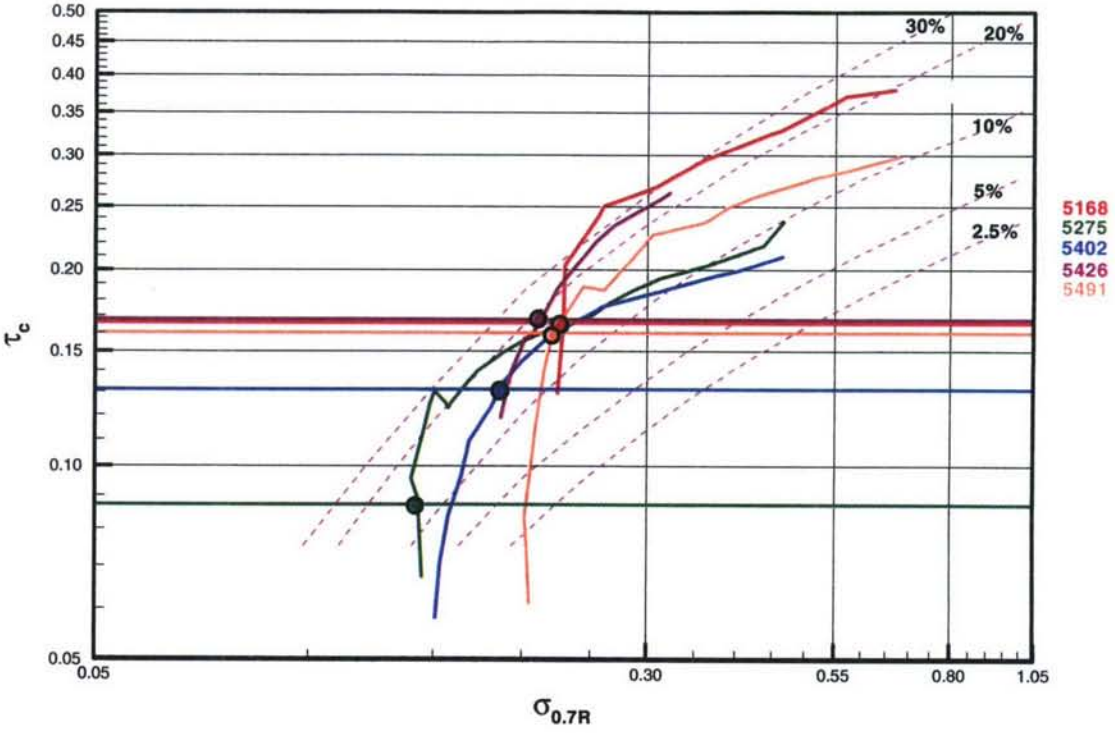

Figure 8. Burrill chart showing thrust breakdown of sample cases in uniform inflow.

Alternative thrust and cavitation number coefficients to those proposed by Burrill were assessed to see if they would allow the data to collapse in a better fashion. For the purposes of this chart, which is to provide a quick guidance as to the recommended blade area needed for a new design, the existing variables seem appropriate. Thickness can impact thrust breakdown performance, but it tends to be a secondary issue when compared to characteristics like ship speed, RPM, area ratio and thrust. The five propellers examined have thickness-to-chord ratios between 4.6 and 4.9 percent except for 5491, which has a ratio of 5.7 percent. The increased thickness could explain why the thrust breakdown envelope for 5491 is shifted slightly to the right relative to the other curves.

INCLINED FLOW

Thrust breakdown calculations for the five propellers were performed for three flow inclination angles. The inflow fields were generated by imposing the first-harmonic inclination inflow on the circumferential mean design inflow. Calculations were performed for shaft angles of three, six and nine degrees. For each combination of propeller and inflow, an unsteady cavitating propeller analysis was performed for a range of advance coefficients and cavitation numbers. The results were used to develop contours of percentage thrust loss for each propeller.

The two-percent thrust loss contours for the three inflow angles are shown in Figures 9 to 11. In the figures, the horizontal lines correspond to the full power thrust coefficient for each propeller. The symbols help to visualize the cavitation numbers where the thrust breakdown contours intersect the design thrust coefficient lines.

The 5275 propeller, at its design thrust coefficient and the nine degree inclination, operates with pressure side cavitation during the low loading portion of each revolution. This was observed full scale for a six degree inflow, but was predicted to be more severe at the higher inclination angle. The PROPCAV software had trouble converging for propeller 5275 at a nin-degree inclination, so the thrust breakdown contour for that propeller in Figure 11 does not extend all the way down to its design thrust coefficient. For higher loadings, the software did not have any problems converging.

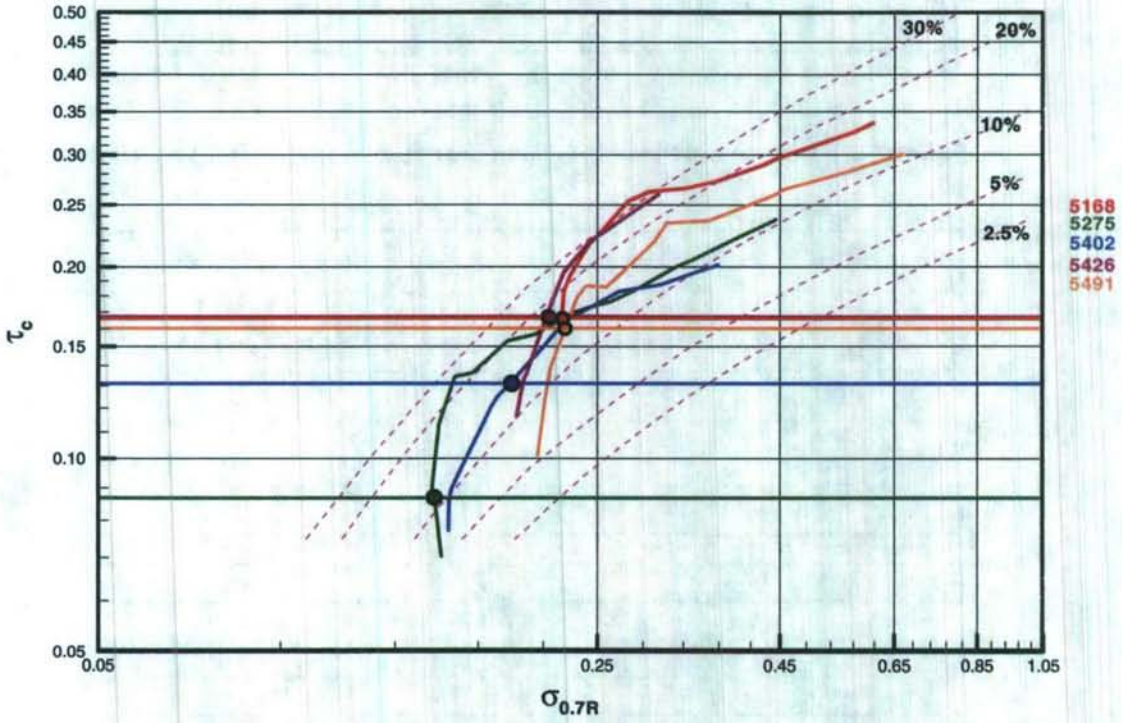

Figure 9. Two-percent thrust loss contours at three degrees of inflow inclination.

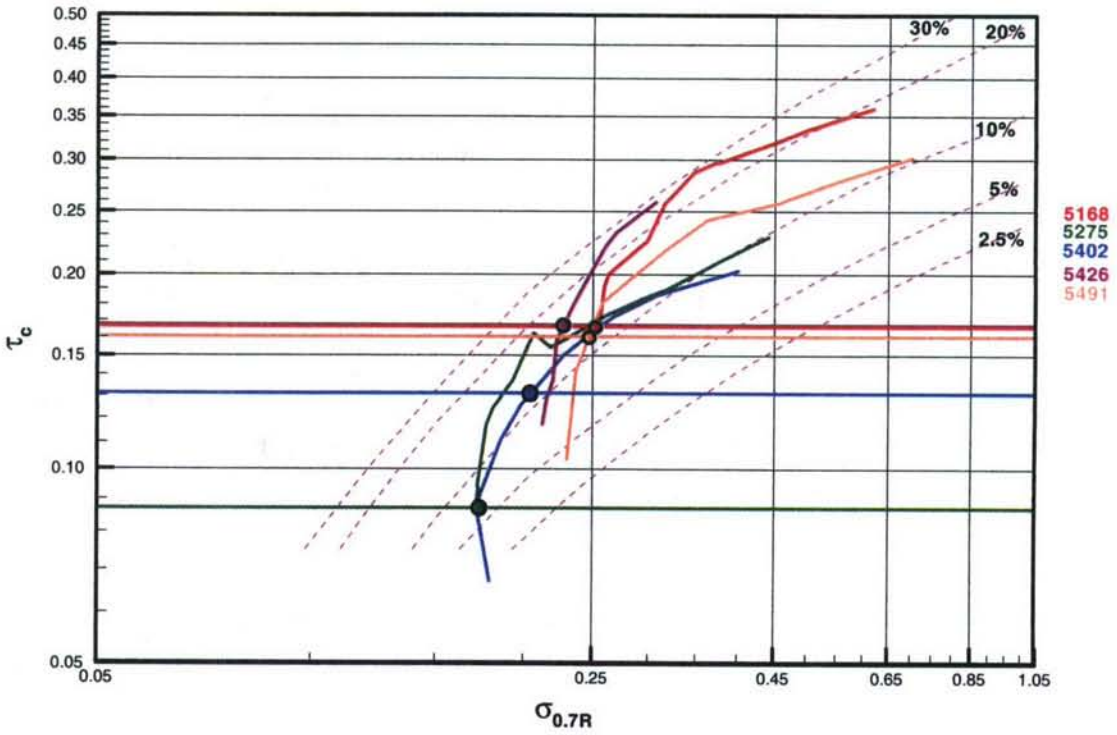

Figure 10. Two-percent thrust loss contours at six degrees of inflow inclination.

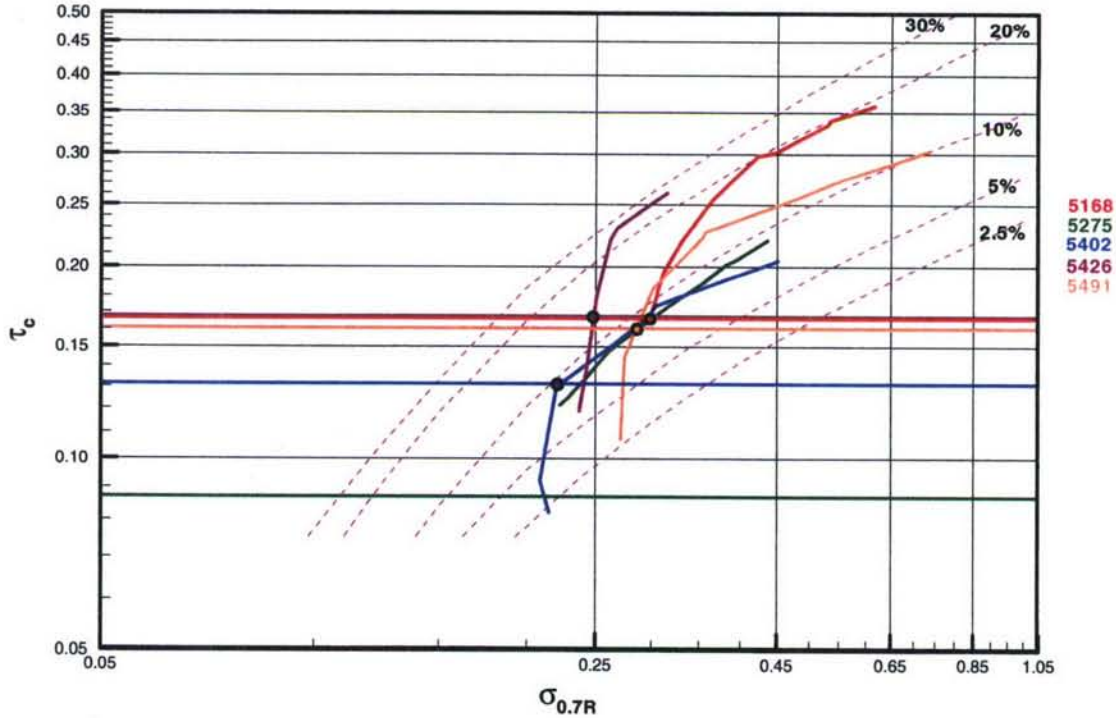

Figure 11. Two-percent thrust loss contours at nine degrees of inflow inclination.

The degradation in cavitation number with inflow inclination is tabulated in Table 2 and shown graphically in Figure 12. The overall trend is that in a non-inclined inflow, thrust breakdown can be avoided along the 15% back cavitation line. As the inflow variations increase to a nine-degree inflow angle, thrust breakdown can be avoided along the 10% back cavitation line. At the design thrust coefficient, the cavitation number ($\sigma_{0.7R}$) increased by approximately 0.05 for the nine-degree inflow incidence over the zero-degree inflow. As the flow angle increases, the 5275 propeller experienced the largest sensitivity of cavitation number to flow inclination angle. PROPCAV was unable to converge for some of the higher shaft angles for propeller 5275. It is not clear if this indicates that designs for low thrust coefficients have more sensitivity to high flow angles or that there is a software issue associated with convergence during pressure side cavitation.

Table 2. Effect of flow inclination on thrust breakdown cavitation number ($\sigma_{0.7R}$) and percent back cavitation at design thrust for five sample propellers.

	0 deg	3 deg	6 deg	9 deg	Design Shaft	Full Power
	Percent Back Cavitation				Angle (deg)	τ_c
5168	0.226 *15%*	0.223 *16%*	0.252 *12%*	0.299 *8%*	9.4	0.166
5275	0.141 *13%*	0.148 *12%*	0.173 *6%*	---	6.1	0.087
5402	0.186 *15%*	0.189 *14%*	0.204 *12%*	0.221 *9%*	9.1	0.131
5426	0.210 *19%*	0.212 *18%*	0.228 *16%*	0.248 *13%*	9.2	0.167
5491	0.220 *15%*	0.226 *14%*	0.247 *12%*	0.286 *8%*	6.0	0.160

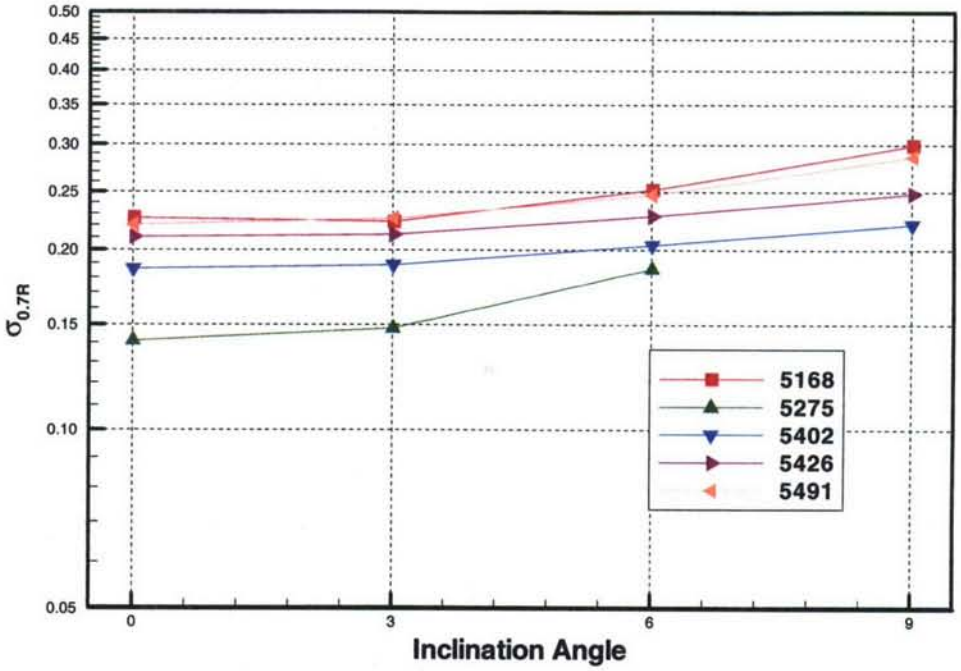

Figure 12. Effect of inflow angle on thrust breakdown cavitation number.

THRUST RECOVERY

As previously discussed, thrust breakdown is defined as losing thrust and torque due to cavitation. When this occurs initially, the propeller RPM can be increased to recover the thrust. However, the increased RPM will also slightly increase the extent of the cavitation. Early in the thrust breakdown process, where one to five percent thrust loss occurs, then to first order, it can be assumed that the reduction in advance coefficient will result in the same thrust coefficient, and the necessary increase in RPM will be inversely related to the square root of the loss in thrust due to cavitation. When more than a five percent thrust loss occurs, a greater RPM increase is necessary.

Blade surface cavitation limits the suction pressure that can be achieved on the blade surface. The cavitation also creates a stagnation point at the closure of the cavity, which further affects the blade pressure distribution. The cavity volume not only disrupts the flow over its own blade, but also disrupts the flow over adjacent blades. Propellers that have significant pressure side concave curvature, like outboard-motor propellers and super-cavitating propellers, can continue to generate thrust at high speeds by increasing RPM. These propellers are even able to generate thrust when the suction side of the blade is completely covered by cavitation. Pressure side concave curvature is not the typical shape for conventional propellers. Conventional propellers may experience unrecoverable thrust breakdown when they encounter between 10 to 20% thrust loss. Therefore, increasing the RPM will not increase the cavitating thrust.

An example of thrust breakdown is shown in Figure 13. The data shown are for propeller 5426 at a cavitation number based on ship speed (σ) of 2.02. If the ship requires 400,000 pounds of thrust to be propelled at this speed, the non-cavitating propeller data predicts an advance coefficient of 0.739 and an RPM of 199. However, cavitation causes the propeller to produce a lower thrust, so the RPM needs to be increased to 204 and an advance coefficient of 0.723. If the ship's resistance increased above 425,000 pounds due to fouling, weight growth or sea condition, the propeller would suffer from complete thrust breakdown, so no amount of RPM increase would produce any additional thrust.

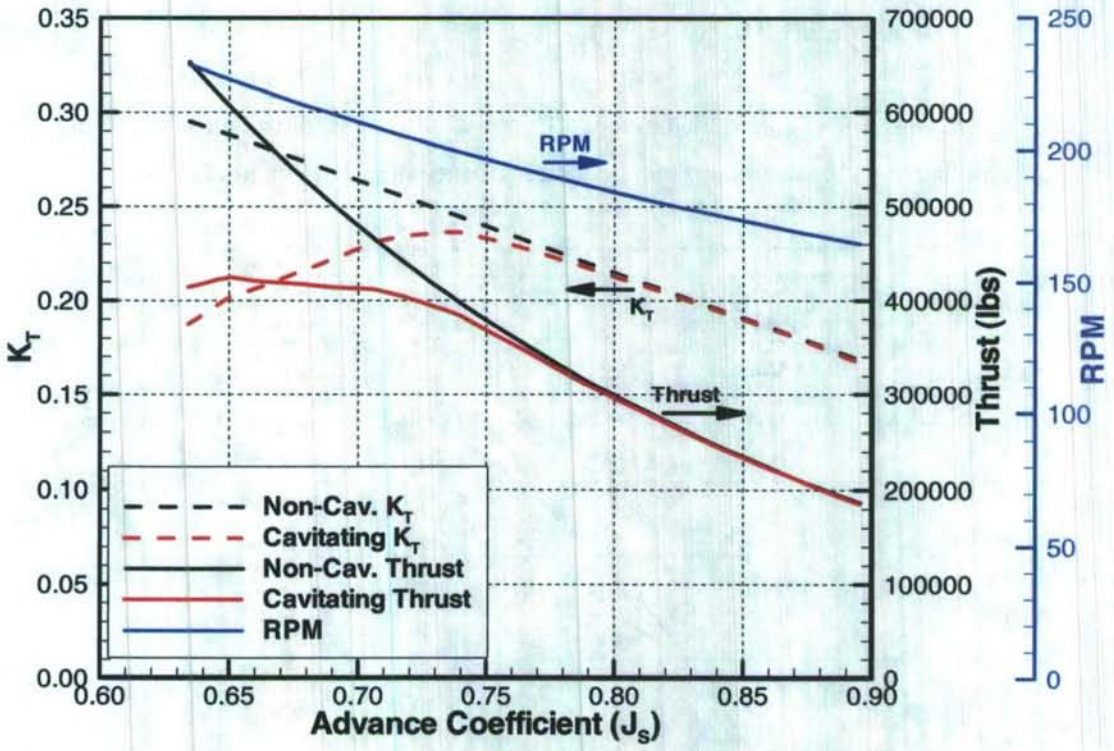

Figure 13. Thrust recovery example.

This study was limited because PROPCAV failed to converge for most conditions with more than ten percent thrust loss. The cavitation number where unrecoverable thrust breakdown occurs could not be determined consistently for the sample propellers.

The contours where five percent thrust loss occurs are consistently at a cavitation number ($\sigma_{0.7R}$) 0.05 less than the value where thrust breakdown began. Typically a five percent thrust loss can be recovered with a two or three percent increase in RPM. This is achievable within the operating envelope of most power plants. It is not recommended to design for more than a five percent thrust loss because of the increased risks of propeller damage due to cavitation.

PROPOSED CRITERIA

For uniform inflow, the proposed thrust coefficient criteria is

$$\tau_c = -0.090 + 1.530*(\sigma_{0.7R}) - 2.100*(\sigma_{0.7R})^2 + 1.200*(\sigma_{0.7R})^3 \quad (1)$$

for cavitation numbers ($\sigma_{0.7R}$) between 0.12 and 0.50. This curve is shown on the Burrill chart in Figure 14. The curve lies very close to the SSPA curve presented by Rutgersson [7]. As the inflow incidence increases, the cavitation number should be modified according to

$$\sigma_{0.7R} = \sigma_{0.7R} + 0.05*(IA / 9)^{2.3} \quad (2)$$

for incidence angles (IA) up to nine degrees. This equation is based on a curve-fit of the relationship between the cavitation number and incidence angle shown in Figure 12.

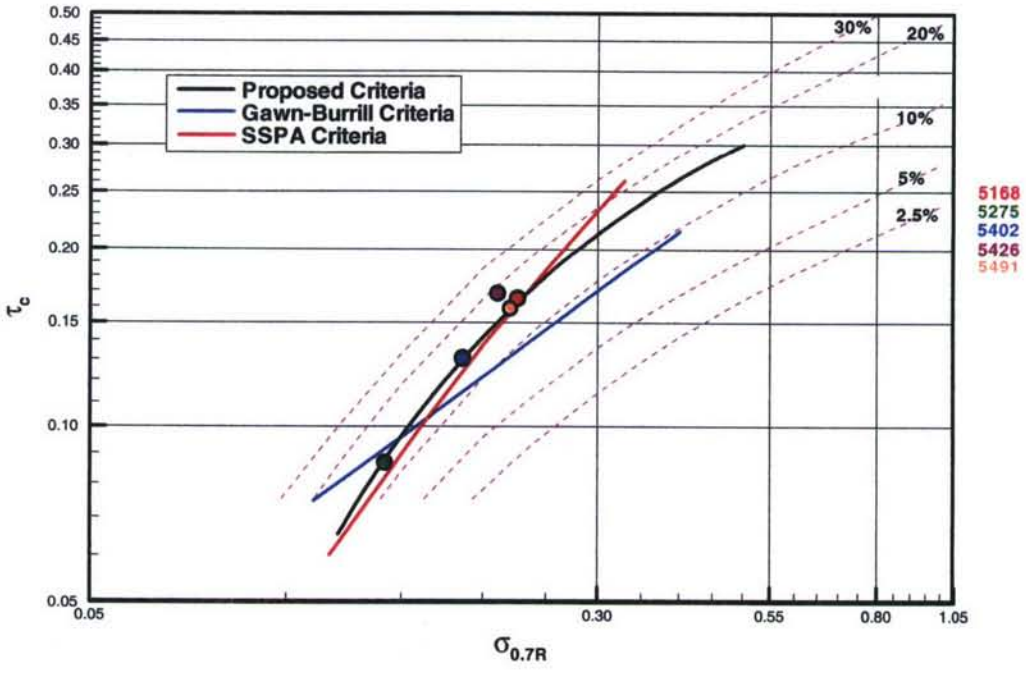

Figure 14. Proposed thrust breakdown criteria.

CONCLUSIONS

A criterion for the selection of blade area to avoid thrust breakdown was developed by analyzing several modern conventional propeller designs. This analysis was performed using propellers that had non-standard blade sections that have typically been used for propeller designs since the early 1990s that maximized their cavitation free operating envelope. This criterion

allows the risk of thrust loss due to cavitation to be quickly assessed for new propeller designs. The new thrust breakdown criterion for uniform inflow propellers lies along the 15% back cavitation curve on the traditional Burrill chart.

The sample propellers were evaluated in a series of flow non-uniformities. A recommendation is made that the cavitation number ($\sigma_{0.7R}$) should be increased by 0.05 in cases with flow non-uniformities comparable to a nine-degree inflow incidence.

At the onset of thrust breakdown, the thrust loss due to cavitation can generally be recovered, by increasing the RPM. In some cases, if more than ten- to twenty-percent of the thrust is lost due to cavitation, unrecoverable thrust breakdown occurs. In these the thrust can not be recovered by increasing the RPM. A five percent thrust loss is generally recoverable with a two or three percent increase in RPM. A five percent thrust loss was found to typically occur at a cavitation number ($\sigma_{0.7R}$) 0.05 lower than the 15% back cavitation thrust loss inception curve.

(THIS PAGE INTENTIONALLY LEFT BLANK)

APPENDIX A PROPELLER GEOMETRY

(THIS PAGE INTENTIONALLY LEFT BLANK)

Table A- 1. Propeller 5168 geometry.

Model Diameter	15.856" (402.7mm)	Number of Blades	5
Expanded Area Ratio	0.830	Chord-wise Camber	Eppler/Shen
Propeller Type	Controllable Pitch	Chord-wise Thickness	Eppler/Shen
Projected Area Ratio	0.66	Full Power J_A	1.20

r/R	c/D	t/D	f/c	Phi (deg)	Skew (deg)	x/D	P/D
0.3000	0.2000	0.0539	-0.0380	49.09	6.2800	0.0111	1.0875
0.3500	0.2370	0.0422	-0.0086	48.55	-0.7542	-0.0069	1.2448
0.4000	0.2760	0.0315	0.0090	47.37	-4.8240	-0.0237	1.3652
0.4500	0.3080	0.0274	0.0178	45.88	-7.3355	-0.0358	1.4579
0.5000	0.3341	0.0252	0.0279	44.46	-8.8650	-0.0437	1.5413
0.6000	0.3854	0.0226	0.0366	41.60	-9.8380	-0.0483	1.6735
0.7000	0.4350	0.0212	0.0332	36.60	-8.1080	-0.0419	1.6333
0.8000	0.4745	0.0195	0.0247	30.87	-3.7838	-0.0302	1.5025
0.8500	0.4818	0.0186	0.0186	28.14	-0.4933	-0.0234	1.4280
0.9000	0.4650	0.0203	0.0119	25.27	3.7838	-0.0165	1.3348
0.9300	0.4305	0.0227	0.0079	23.31	6.9225	-0.0123	1.2588
0.9500	0.3900	0.0229	0.0054	21.73	9.2973	-0.0096	1.1892
0.9700	0.3254	0.0205	0.0030	19.79	11.9267	-0.0068	1.0966
0.9900	0.2056	0.0131	0.0009	17.40	14.8344	-0.0039	0.9744
1.0000	0.0000	0.0000	0.0000	15.99	16.4000	-0.0025	0.9000

Table A- 2. Propeller 5275 geometry.

Model Diameter	16.00" (406.4mm)	Number of Blades	6
Expanded Area Ratio	1.175	Chord-wise Camber	Eppler/Shen
Propeller Type	Fixed Pitch	Chord-wise Thickness	Eppler/Shen
Projected Area Ratio	0.88	Full Power J_A	1.23

r/R	c/D	t/D	f/c	Phi (deg)	Skew (deg)	x/D	P/D
0.2500	0.3780	0.0348	-0.0083	60.38	-6.0000	-0.0144	1.3812
0.3000	0.3917	0.0327	0.0188	56.96	-0.3747	-0.0011	1.4493
0.3500	0.4050	0.0314	0.0199	53.44	4.5000	0.0122	1.4827
0.4000	0.4179	0.0304	0.0191	49.98	9.0000	0.0241	1.4963
0.5000	0.4400	0.0282	0.0205	43.61	16.6502	0.0452	1.4963
0.6000	0.4554	0.0251	0.0210	38.19	23.2501	0.0635	1.4827
0.7000	0.4620	0.0214	0.0208	33.67	28.8748	0.0810	1.4649
0.8000	0.4466	0.0179	0.0195	29.79	33.7501	0.0978	1.4388
0.9000	0.3724	0.0145	0.0142	26.06	38.7319	0.1186	1.3825
0.9500	0.2872	0.0124	0.0085	23.36	41.7698	0.1362	1.2890
0.9750	0.2105	0.0097	0.0051	21.28	43.4503	0.1486	1.1930
0.9900	0.1426	0.0067	0.0030	19.81	44.4902	0.1570	1.1202
1.0000	0.0000	0.0000	0.0016	18.75	45.1800	0.1630	1.0666

Table A- 3. Propeller 5402 geometry.

Model Diameter	16.00" (406.4mm)	Number of Blades	5
Expanded Area Ratio	0.741	Chord-wise Camber	Eppler/Shen
Propeller Type	Fixed Pitch	Chord-wise Thickness	Eppler/Shen
Projected Area Ratio	0.60	Full Power J_A	0.86

r/R	c/D	t/D	f/c	Phi (deg)	Skew (deg)	x/D	P/D
0.1825	0.2209	0.0572	-0.0043	59.31	0.0000	0.0016	0.9662
0.2000	0.2275	0.0508	-0.0026	57.92	0.0137	0.0016	1.0023
0.2500	0.2458	0.0393	0.0062	54.17	0.2043	0.0016	1.0878
0.3000	0.2628	0.0341	0.0150	50.52	0.6194	0.0016	1.1440
0.4000	0.2937	0.0279	0.0190	43.08	2.1230	0.0016	1.1751
0.5000	0.3215	0.0232	0.0168	36.42	4.5245	0.0016	1.1591
0.6000	0.3384	0.0195	0.0152	31.02	7.8238	0.0016	1.1334
0.7000	0.3353	0.0161	0.0148	26.64	12.0210	0.0016	1.1031
0.8000	0.3100	0.0135	0.0149	22.96	17.1161	0.0016	1.0646
0.8500	0.2865	0.0122	0.0147	21.29	20.0004	0.0016	1.0404
0.9000	0.2508	0.0105	0.0139	19.58	23.1091	0.0016	1.0057
0.9500	0.1910	0.0080	0.0112	17.43	26.4423	0.0016	0.9372
0.9800	0.1272	0.0053	0.0060	15.80	28.5500	0.0016	0.8715
1.0000	0.0000	0.0000	0.0000	14.45	30.0000	0.0016	0.8094

Table A- 4. Propeller 5426 geometry.

Model Diameter	16.506" (419.3mm)	Number of Blades	5
Expanded Area Ratio	0.724	Chord-wise Camber	Eppler/Shen
Propeller Type	Controllable Pitch	Chord-wise Thickness	Eppler/Shen
Projected Area Ratio	0.63	Full Power J_A	0.78

r/R	c/D	t/D	f/c	Phi (deg)	Skew (deg)	x/D	P/D
0.2500	0.1242	0.0730	-0.0416	35.49	4.0857	0.0065	0.5600
0.3000	0.1545	0.0527	-0.0053	38.20	-0.7000	-0.0021	0.7417
0.4000	0.2330	0.0300	0.0300	41.01	-8.8454	-0.0178	1.0928
0.5000	0.2934	0.0237	0.0328	37.35	-12.1737	-0.0321	1.1990
0.6000	0.3493	0.0211	0.0287	32.19	-12.4649	-0.0400	1.1867
0.7000	0.3964	0.0192	0.0237	26.78	-10.3777	-0.0410	1.1101
0.8000	0.4248	0.0176	0.0199	21.40	-4.0997	-0.0375	0.9851
0.9000	0.3831	0.0187	0.0177	16.57	7.1093	-0.0290	0.8410
0.9500	0.2941	0.0210	0.0169	14.43	14.5963	-0.0225	0.7682
0.9750	0.2151	0.0177	0.0166	13.43	18.7203	-0.0189	0.7316
0.9900	0.1399	0.0113	0.0164	12.85	21.2862	-0.0165	0.7096
1.0000	0.0000	0.0000	0.0164	12.47	23.0343	-0.0148	0.6948
0.2500	0.1242	0.0730	-0.0416	35.49	4.0857	0.0065	0.5600

Table A- 5. Propeller 5491 geometry.

Model Diameter	10.673" (271.1mm)	Number of Blades	5
Expanded Area Ratio	0.837	Chord-wise Camber	Eppler/Shen
Propeller Type	Fixed Pitch	Chord-wise Thickness	Eppler/Shen
Projected Area Ratio	0.64	Full Power J_A	1.04

r/R	c/D	t/D	f/c	Phi (deg)	Skew (deg)	x/D	P/D
0.2000	0.2725	0.0581	-0.0232	59.87	0.0000	-0.0023	1.0828
0.2500	0.2901	0.0437	-0.0072	58.77	-2.4973	-0.0058	1.2952
0.3000	0.3046	0.0393	0.0062	56.22	-4.4893	-0.0093	1.4087
0.4000	0.3290	0.0343	0.0239	49.66	-6.9572	-0.0143	1.4798
0.5000	0.3462	0.0291	0.0294	43.32	-7.4038	-0.0152	1.4811
0.6000	0.3547	0.0241	0.0298	37.84	-5.8289	-0.0119	1.4644
0.7000	0.3565	0.0203	0.0270	32.93	-2.2327	-0.0044	1.4241
0.8000	0.3527	0.0183	0.0237	27.70	3.3849	0.0062	1.3193
0.8500	0.3451	0.0177	0.0207	24.96	6.9517	0.0120	1.2427
0.9000	0.3276	0.0170	0.0161	22.10	11.0239	0.0176	1.1481
0.9500	0.2911	0.0157	0.0090	19.41	15.5527	0.0227	1.0513
0.9800	0.2491	0.0146	0.0039	17.96	17.7008	0.0245	0.9980
1.0000	0.0000	0.0000	0.0000	17.06	19.8427	0.0266	0.9643

(THIS PAGE INTENTIONALLY LEFT BLANK)

APPENDIX B PROPELLER OPEN WATER PREDICTIONS

(THIS PAGE INTENTIONALLY LEFT BLANK)

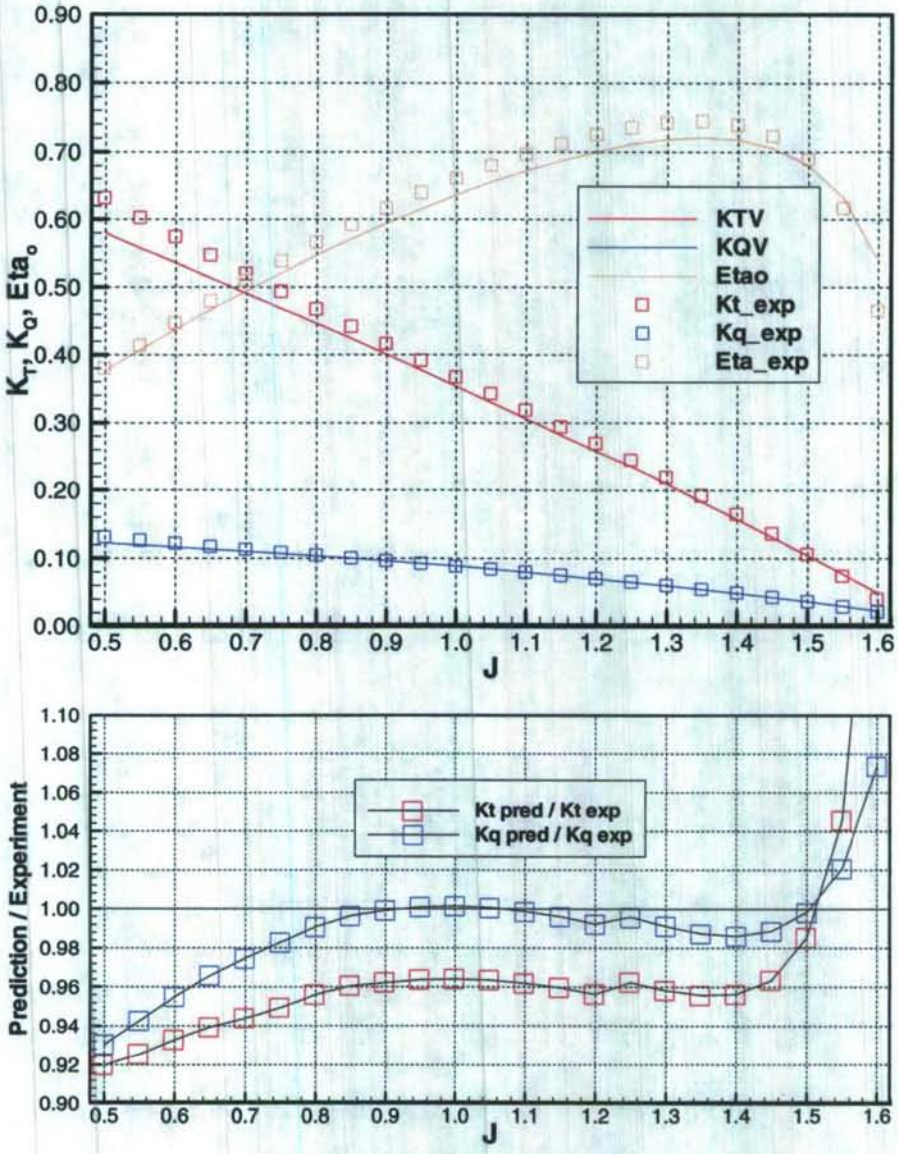

Figure B- 1. Propeller 5168 open water prediction.

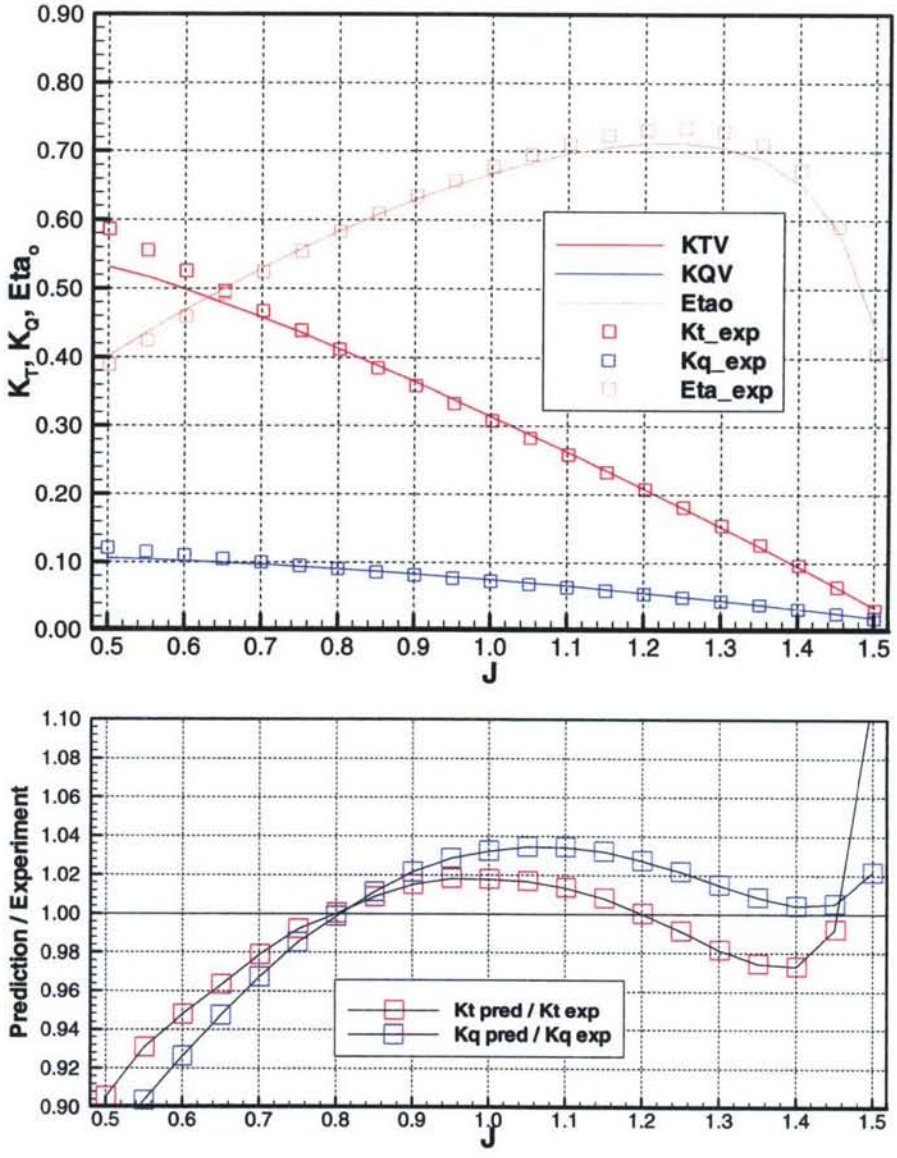

Figure B- 2. Propeller 5275 open water prediction.

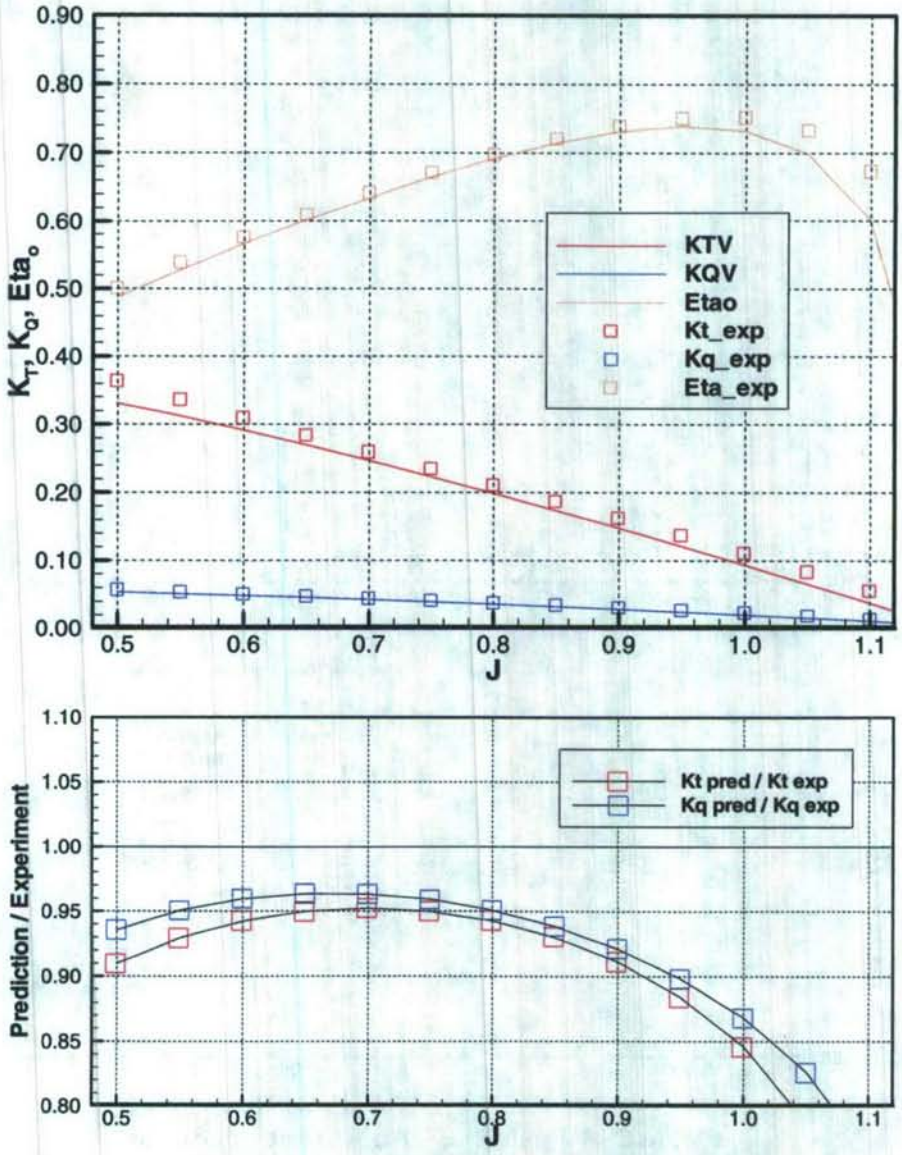

Figure B- 3. Propeller 5402 open water prediction.

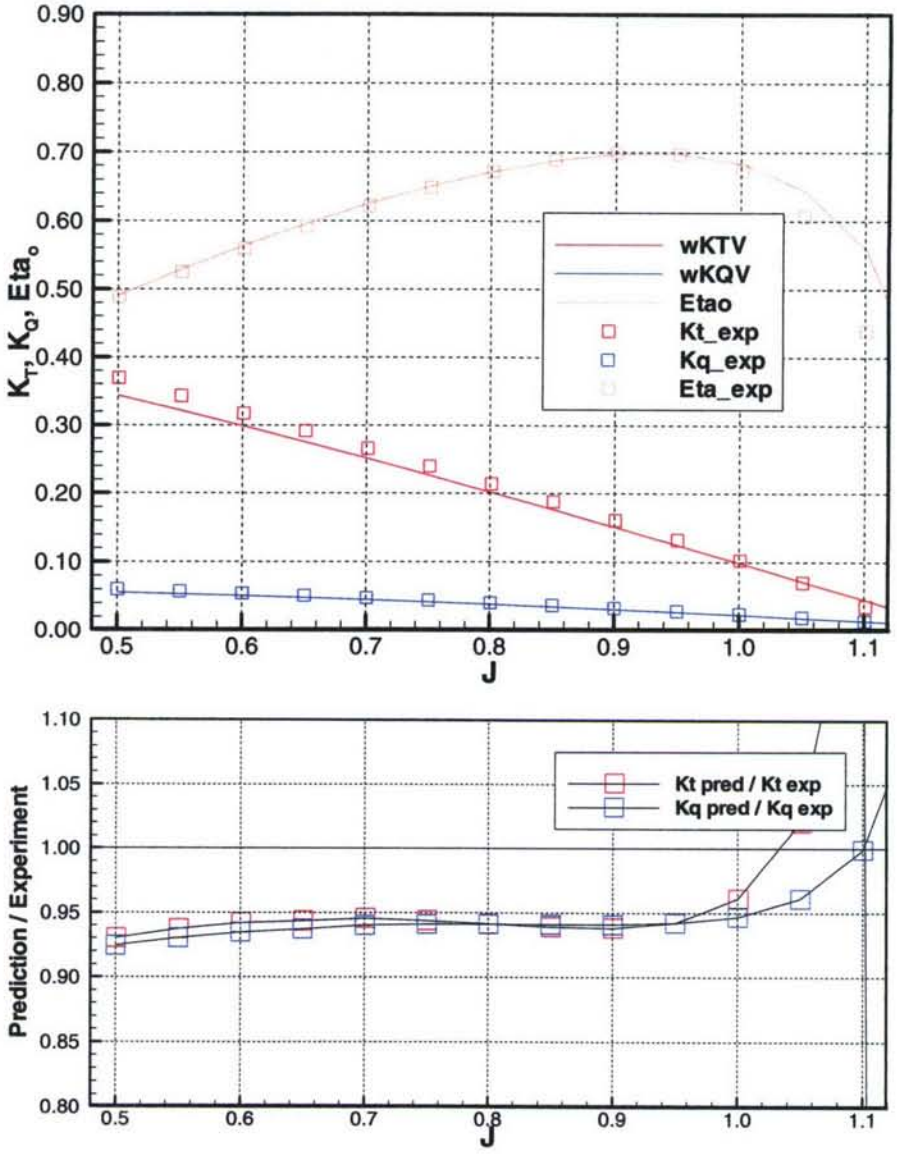

Figure B- 4. Propeller 5426 open water prediction.

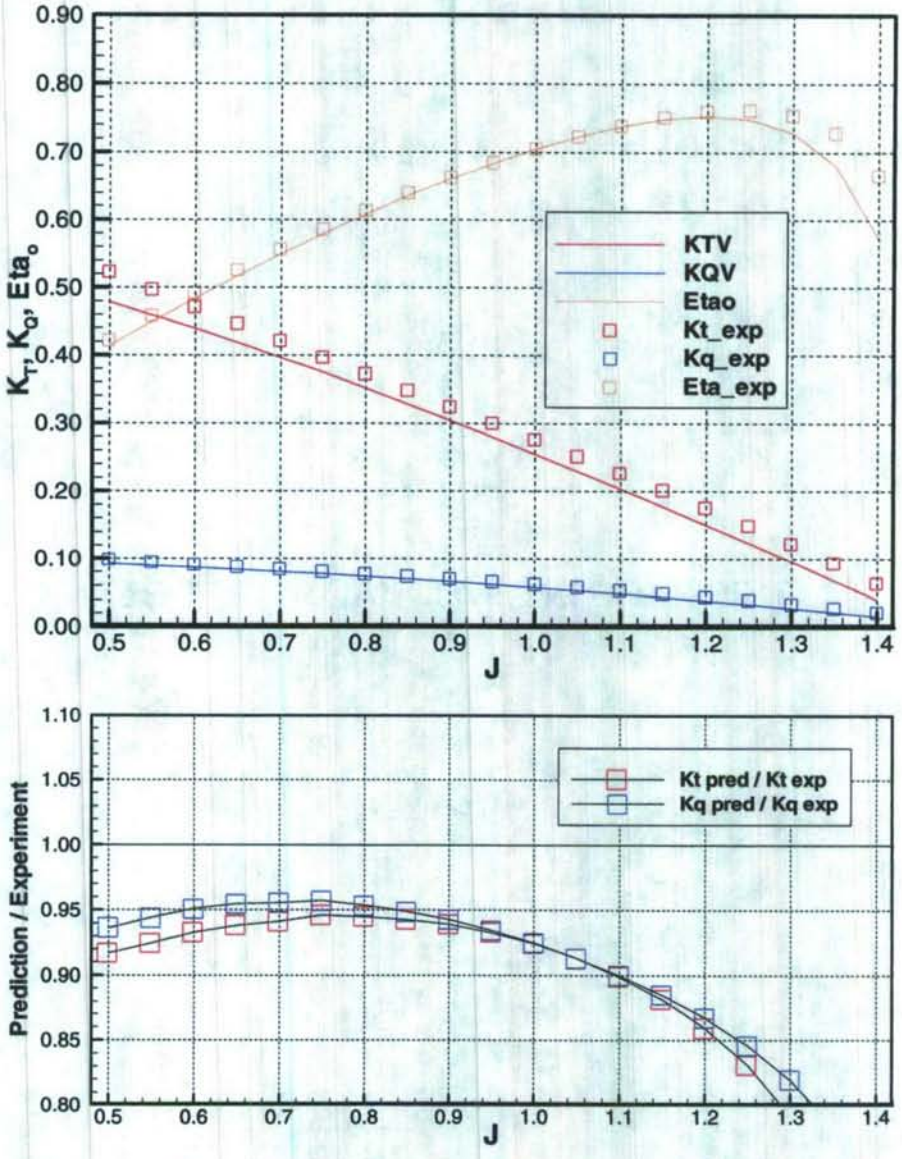

Figure B- 5. Propeller 5491 open water prediction.

(THIS PAGE INTENTIONALLY LEFT BLANK)

APPENDIX C THRUST LOSS MAPS

(THIS PAGE INTENTIONALLY LEFT BLANK)

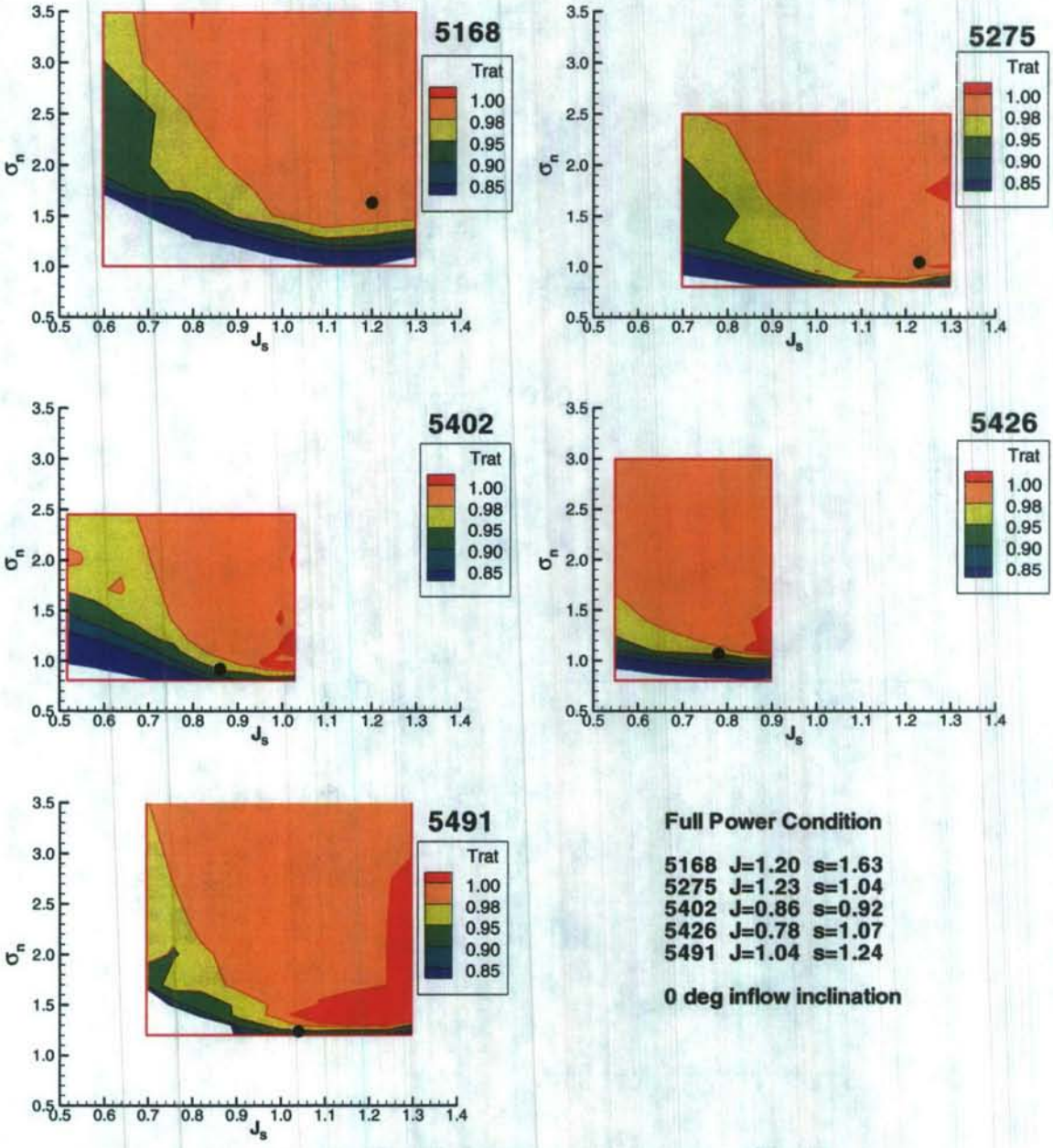

Figure C- 1. Thrust loss maps for zero-degree inflow inclination.

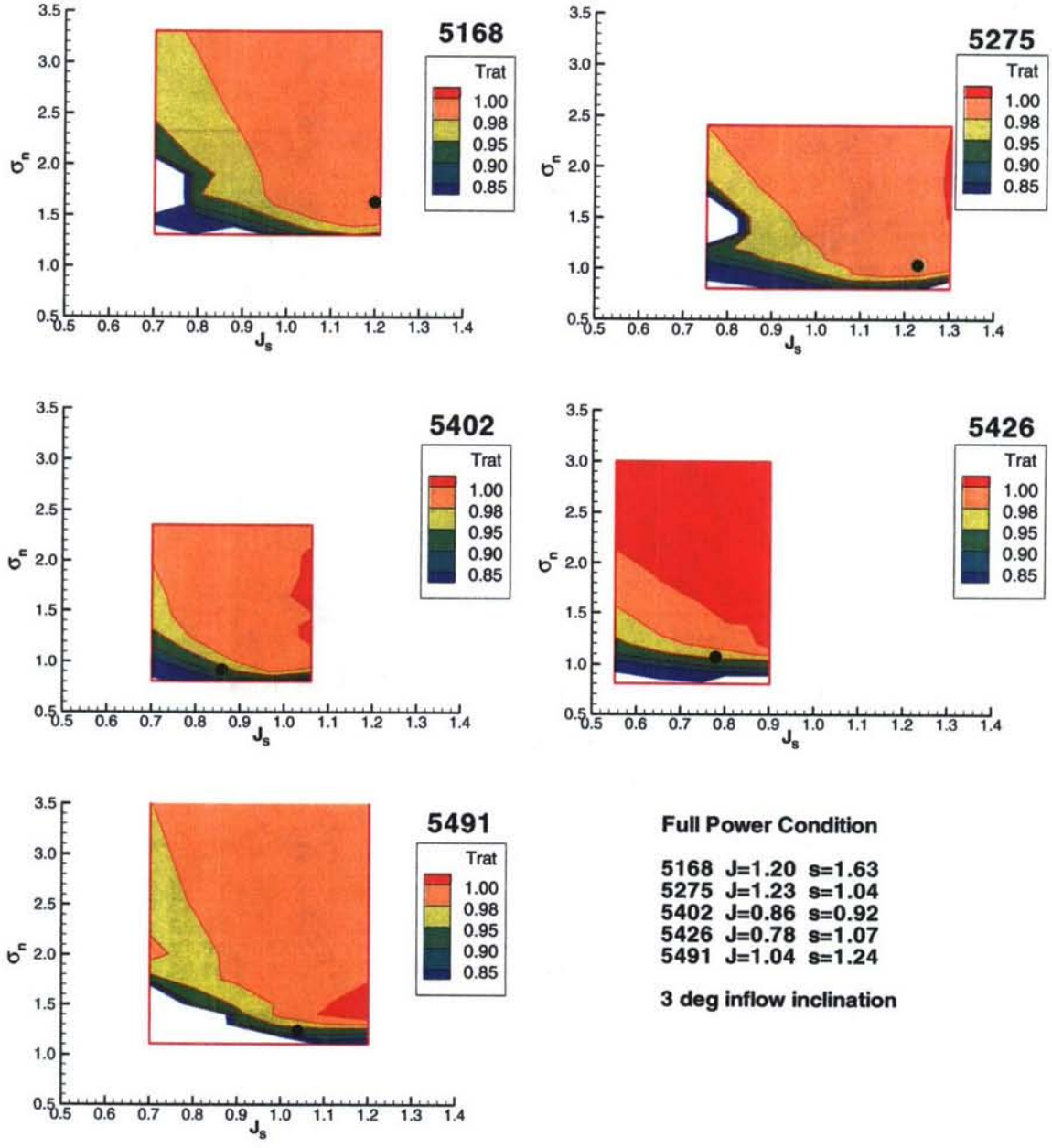

Figure C- 2. Thrust loss maps for three-degree inflow inclination.

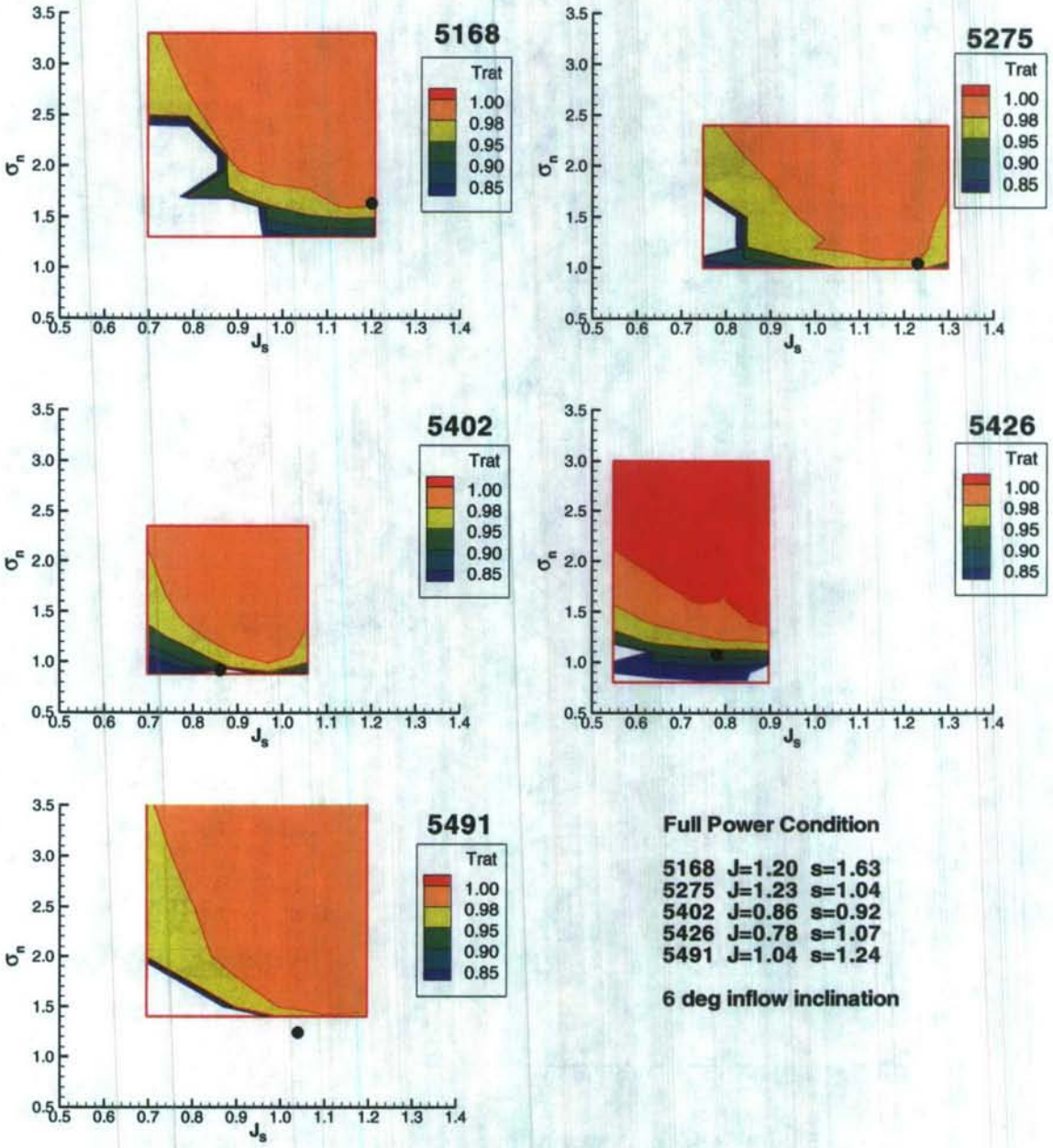

Figure C- 3. Thrust loss maps for six-degree inflow inclination.

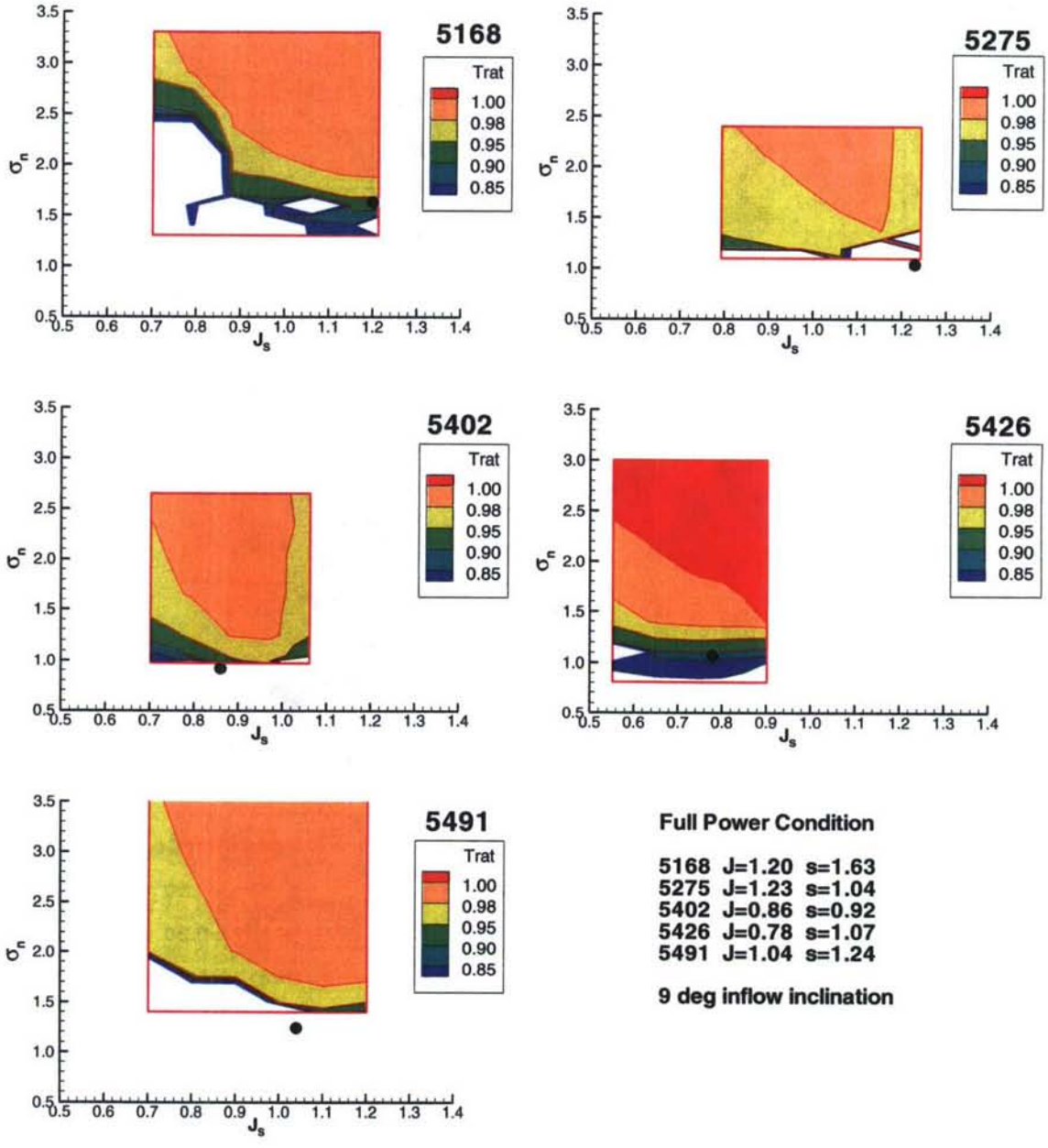

Figure C- 4. Thrust loss maps for nine-degree inflow inclination.

REFERENCES

1. International Towing Tank Conference, "ITTC – Recommended Procedures and Guidelines" 22nd ITTC Propulsion Committee Report, Seoul, Korea, 1999.

2. Burrill, L. C. and A. Emerson, "Propeller Cavitation: Further Tests on 16in. Propeller Models in the King's College Cavitation Tunnel," Transactions of the North East Coast Institution of Engineers and Ship Builders, Vol. 78 pp. 295-320, 1963-64.

3. Burrill, L. C., "Developments in Propeller Design and Manufacture for Merchant Ships," *Transactions*, Institute of Marine Engineers, London, Vol. 55, 1943.

4. Parsons, C.A. and S.S. Cook, "Investigations into the Causes of Corrosion or Erosion of Propellers," *Transactions*, Institute of Naval Architects, Volume 61, 1919.

5. Barnaby, S.W. "On the Formation of Cavities in Water by Screw Propellers at High Speeds," *Transactions*, Institute of Naval Architects, Volume 39, 1897.

6. Gawn, R. W. and L. C. Burrill, "Effect of Cavitation on the Performance of a Series of 16 inch Model Propellers," Royal Institute of Naval Architects, 1957.

7. Rutgersson, O., "Cavitation on High Speed Propellers in Oblique Flow-Influence of Propeller Design and Interaction with Ship Hull," 13th Symposium on Naval Hydrodynamics, Tokyo, Japan, Oct., 1980.

8. Bailar J.W., S.D. Jessup and Y.T. Shen, "Improvement of Surface Ship Propeller Cavitation Performance Using Advanced Blade Sections," 23rd American Towing Tank Conference, New Orleans, USA, 1992.

9. Brocket, T. E., "Minimum Pressure Envelopes for Modified NACA-66 Sections with NACA a=0.8 Camber and Buships Type I and Type II Sections," DTNSRDC Report 1780, Feb 1966.

10. Kinnas, S. A., P. E. Griffin, and A. C. Mueller, "Computational Tools for the Analysis and Design of High-Speed Propulsors," The International CFD Conference, Ulsteinvik Norway, May 1997.

11. Lee, H., H. Sun, and S.A. Kinnas, "PROPCAV (Version 2.3) User's Manual and Documentation," Department of Civil, Architectural and Environmental Engineering Report 07-1, January 2007.

12. Young, Y.L. and S.A. Kinnas, "Numerical Modeling of Supercavitating Propeller Flows," *Journal of Ship Research*, 47(1):48-62, March 2003.

13. Bosschers, J., M. Zijlstra, and G. Vaz, "PROCAL V1.0 User Guide," MARIN Report 18384-8-SP, May 2006.

14. Lindau, J.W., D.A. Boger, R.B. Medvitz and R.F. Kunz, "Propeller Cavitation Breakdown Analysis," Journal of Fluid Engineering, Volume 127, Issue 5, pp 995-1002, September 2005.

15. Rhee, S.H., T. Kawamura, and H. Li, "Propeller Cavitation Study using an Unstructured Grid Based Navier-Stokes Solver," Journal of Fluid Engineering, Volume 127, Issue 5, pp. 986-994, September 2005.

16. Watanabe, T., T. Kawamura, Y. Takekoshi, M. Maeda, and S.H. Rhee, "Simulation of Steady and Unsteady Cavitation on Marine Propeller using a RANS CFD Code," Fifth International Symposium on Cavitation (CAV2003), Osaka, Japan, November 2003.

17. Shen, Y. T. and R. Eppler, "Wing Sections for Hydrofoils – Part 2: Nonsymmetrical Profiles," Journal of Ship Research, Vol. 25, pp. 191-200, September 1981.

18. Jessup S. D. and H.-C. Wang, "Propeller Design and Evaluation for a High Speed Patrol Boat Incorporating Iterative Analysis With Panel Code," Propellers/Shafting '97 Symposium, Society of Naval Architects and Marine Engineers, Virginia Beach, VA, Sep 1997.

INITIAL DISTRIBUTION

EXTERNAL DISTRIBUTION

ORG.	NAME
NAVSEA	
05Z11	Schumann
PMS 385	Goldberg, Liese
	Davison
PEO SHIPS	(1)
N42	Kaskin
ONR 333	Kim
DTIC	

CENTER DISTRIBUTION

CODE	NAME (Copies)
2240	Kennell
2240	Lamb
2410	Anderson
2420	Fung
3452	NSWCCD Library
5010	(w/o enclosure)
5030	Jessup
5060	Walden
5200	Karafiath
5200	Hurwitz
5400	Black
5400	Gorski


UNITED STATES NAVY
SURFACE WARFARE CENTER